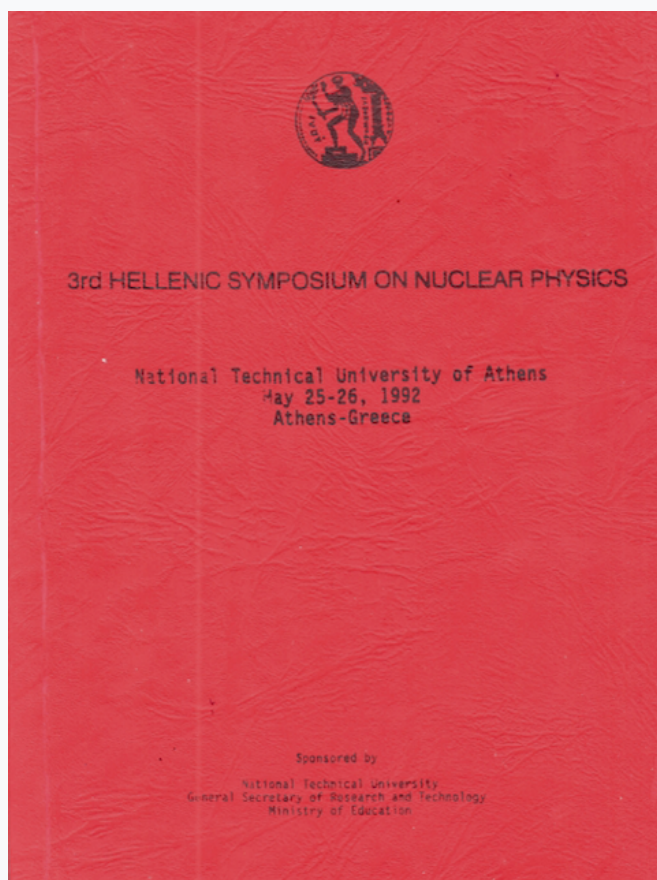


HNPS Advances in Nuclear Physics

Vol 3 (1992)

HNPS1992



Two body density matrix of model nuclear matter

E. Mavromanatis, M. Petraki, J. W. Clark

doi: [10.12681/hnps.2376](https://doi.org/10.12681/hnps.2376)

To cite this article:

Mavromanatis, E., Petraki M., & Clark, J. W. (2019). Two body density matrix of model nuclear matter. *HNPS Advances in Nuclear Physics*, 3, 88–103. <https://doi.org/10.12681/hnps.2376>

TWO-BODY DENSITY MATRIX OF MODEL NUCLEAR MATTER*

E. MAVROMMATIS AND M. PETRAKI

*Physics Department, Division of Nuclear and Particle Physics
University of Athens, Panepistimioupoli, 15771 Athens, Greece*

J. W. CLARK

*McDonnell Center for the Space Sciences and Department of Physics
Washington University, St. Louis, MO 63130 USA*

Abstract

A lowest-cluster-order variational calculation of the half-diagonal two-body density matrix $\rho_2(r_1, r_2, r'_1)$ and the corresponding generalized momentum distribution $n(p, Q)$ is performed for three representative models of nuclear matter containing central correlations. Dynamical correlations produce significant deviations from the results for a noninteracting Fermi gas. Calculations are in progress that include higher-order cluster corrections as well as state-dependent correlations.

1. Introduction

In this paper, we present the results of a variational calculation of the half-diagonal two-body density matrix $\rho_2(r_1, r_2, r'_1)$ for the ground state of symmetrical nuclear matter. We choose certain simplified models of this system that incorporate state-independent correlations, and restrict the calculation to leading, two-body cluster order.

There is increasing interest in the determination of the two-body density matrix of finite nuclei. This interest is stimulated by the fact that proper interpretation of a range of recent or planned experiments, in new or developing facilities, hinges on a more quantitative understanding of the propagation of ejected nucleons and their final-state interactions (FSI). Attention is focused on inclusive quasielastic (e, e') scattering [1] as well as exclusive quasielastic ($e, e'N$) [2] and ($e, e'2N$) scatterings. In these electronuclear processes, FSI can have a significant impact at low energy transfer even for beam energies in the multi-GeV region. Reliable extraction of the momentum distributions, spectral functions, and transparency from the experimental data requires an accurate accounting of final-state effects. In addition to electron scattering, FSI are involved in proton scattering ($p, 2p$) [3] and pion absorption [4] experiments. As we

*Presented by E. Mavrommatis

progress beyond mean-field, optical-model descriptions, theoretical treatments of FSI are found to involve, as input, the diagonal and half-diagonal portions of the two-body density matrix. Notable examples include the extensions of Glauber theory [5,6], adaptation of Silver's hard-core perturbation theory to the nuclear medium [7], and other approaches under current discussion [8,9].

There is an additional motivation for explicit calculation of $\rho_2(\mathbf{r}_1, \mathbf{r}_2, \mathbf{r}'_1)$ and $n(\mathbf{p}, \mathbf{Q})$. For strongly interacting Bose systems, particularly liquid ^4He , recent formal results [10] along with older findings [11] have established the key role played by these quantities in the ω^2 sum rule for the density-density operator, as well as analogous sum rules for the particle-particle and density-particle operators. It is to be expected that $\rho_2(\mathbf{r}_1, \mathbf{r}_2, \mathbf{r}'_1)$ will likewise be an essential ingredient of the corresponding sum rules for Fermi systems including nuclear matter. Such sum rules should provide valuable information on the nature and importance of single-particle and collective excitations of the nuclear medium.

The half-diagonal two-body density matrix for a system of A particles is defined by

$$\rho_2(\mathbf{r}_1, \mathbf{r}_2, \mathbf{r}'_1) = A(A-1) \int \Psi^*(\mathbf{r}_1, \mathbf{r}_2, \mathbf{r}_3, \dots) \Psi(\mathbf{r}'_1, \mathbf{r}_2, \mathbf{r}_3, \dots) d\mathbf{r}_3 \dots d\mathbf{r}_A . \quad (1)$$

(Spin and isospin indices are suppressed, and a sum over all spin/isospin variables is implied.) The Fourier transform of this function defines the generalized momentum distribution

$$n(\mathbf{p}, \mathbf{Q}) = \frac{\rho}{A} \int \rho_2(\mathbf{r}_1, \mathbf{r}_2, \mathbf{r}'_1) e^{-i\mathbf{p}(\mathbf{r}_1 - \mathbf{r}'_1)} e^{-i\mathbf{Q}(\mathbf{r}'_1 - \mathbf{r}_2)} d\mathbf{r}_1 d\mathbf{r}_2 d\mathbf{r}'_1 . \quad (2)$$

In expression (1), Ψ is the normalized wave function of the ground state. It is assumed that the system has uniform density ρ . In the full-diagonal case ($\mathbf{r}_1 = \mathbf{r}'_1$), Eq. (1) reduces to

$$\rho_2(\mathbf{r}_1, \mathbf{r}_2, \mathbf{r}_1) = \rho^2 g(r_{12}) , \quad (3)$$

and, summing over \mathbf{p} in Eq. (2), we arrive at the so-called \mathbf{p} sum rule,

$$\frac{1}{A} \sum_{\mathbf{p}} n(\mathbf{p}, \mathbf{Q}) = A \delta_{\mathbf{Q}0} + \rho \int [g(r_{12}) - 1] e^{-i\mathbf{Q}\mathbf{r}_{12}} d\mathbf{r}_{12} = A \delta_{\mathbf{Q}0} + [S(\mathbf{Q}) - 1] , \quad (4)$$

where $S(\mathbf{Q})$ is the static structure function.

The sequential relation in configuration space,

$$\int \rho_2(\mathbf{r}_1, \mathbf{r}_2, \mathbf{r}'_1) d\mathbf{r}_2 = (A-1) \rho_1(\mathbf{r}_1, \mathbf{r}'_1) , \quad (5)$$

relates $\rho_2(\mathbf{r}_1, \mathbf{r}_2, \mathbf{r}'_1)$ with the one-body density matrix $\rho_1(\mathbf{r}_1, \mathbf{r}'_1)$. The corresponding condition in momentum space,

$$n(\mathbf{p}, \mathbf{Q}=0) = (A-1)n(p) \quad (6)$$

relates $n(\mathbf{p}, \mathbf{Q})$ to the momentum distribution $n(p)$.

The one-body density matrix $\rho_1(\mathbf{r}_1, \mathbf{r}'_1)$ and the momentum distribution $n(p)$ have been studied extensively in the case of nuclear matter [12-15] and finite nuclei [16]. Three simple prescriptions for estimating the half-diagonal density matrix of quantum fluids are available in the literature [17]. Recently, thorough microscopic analyses of the two-body density matrices of strongly-interacting Bose [18] and Fermi [19] systems have been undertaken within the variational approach and approximate calculations performed for liquid ${}^4\text{He}$ and liquid ${}^3\text{He}$ using hypernetted-chain (HNC) techniques. A preliminary report on evaluation of $\rho_2(\mathbf{r}_1, \mathbf{r}_2, \mathbf{r}'_1)$ in liquid ${}^4\text{He}$ within the path-integral Monte Carlo method has been given [20] and further computations involving stochastic procedures are in progress [21]. However, to the best of our knowledge there is as yet no quantitative treatment of $\rho_2(\mathbf{r}_1, \mathbf{r}_2, \mathbf{r}'_1)$ and $n(\mathbf{p}, \mathbf{Q})$ in nuclear problems.

Our calculation for $\rho_2(\mathbf{r}_1, \mathbf{r}_2, \mathbf{r}'_1)$ in nuclear matter may give a crude picture of the corresponding quantity in medium-to-heavy nuclei. A better description may be obtained with an appropriate local-density approximation, as has been proposed for the momentum distribution of finite nuclei in Ref. [22].

The microscopic evaluation of $\rho_2(\mathbf{r}_1, \mathbf{r}_2, \mathbf{r}'_1)$ and $n(\mathbf{p}, \mathbf{Q})$ can be pursued in terms of different theoretical approaches to the ground state of nuclear matter: stochastic, perturbative, and variational. The variational treatment can be supplemented, as necessary, with corrections determined within correlated-basis-functions (CBF) theory. Following the variational approach [23], we have carried out a low-order calculation as described in Sec. 2. Numerical results are displayed and discussed in Sec. 3, and some prospects for improvements upon the present calculation are indicated in Sec. 4.

2. Lowest-Order Variational Calculation

Our calculation is based on the microscopic analysis of the half-diagonal two-body density $\rho_2(\mathbf{r}_1, \mathbf{r}_2, \mathbf{r}'_1)$ developed for Fermi fluids by Ristig and Clark [19] within the variational CBF theory [24]. The Ristig-Clark analysis is patterned after a more elaborate study [18] of the Bose two-body density matrix and exploits techniques and results developed some years ago [25] for the one-body density matrix and momentum distribution of a quantum fluid. For the uniform Fermi system, the ground-state wave function is approximated by a trial wave function of Jastrow-Slater form

$$\Psi = N^{-1} \prod_{i < j}^A f(r_{ij}) \Phi \quad (7)$$

Here, Φ is a Slater determinant of A plane-wave orbitals filling the Fermi sea up to a wave number k_F related to the density by $\rho = \nu k_F^3 / 6\pi^2$, where ν is the single-particle

level degeneracy, $f(r_{ij})$ is the Jastrow two-body correlation function, and N is a normalization constant. Considerations begin with the generalized momentum distribution $n(\mathbf{p}, \mathbf{Q})$ corresponding to $\rho_2(\mathbf{r}_1, \mathbf{r}_2, \mathbf{r}'_1)$ through Eq. (2). This quantity may be decomposed as follows

$$n(\mathbf{p}, \mathbf{Q}) = \delta_{Q0}(A-1)n(p) + (1-\delta_{Q0})\langle \Psi | N(\mathbf{p}, \mathbf{Q}) | \Psi \rangle, \quad (8)$$

where the first term, henceforth denoted $n_o(\mathbf{p}, \mathbf{Q})$ contains no statistical nor dynamical effects other than those contained in the momentum distribution $n(p)$, and the remainder involves the expectation value of a non-self-adjoint operator $N(\mathbf{p}, \mathbf{Q})$. In terms of the usual particle creation and destruction operators a_k^\dagger and a_k and density operators ρ_Q , we have

$$2N(\mathbf{p}, \mathbf{Q}) = \rho_Q a_{\mathbf{p}-\mathbf{Q}}^\dagger a_{\mathbf{p}} + a_{\mathbf{p}-\mathbf{Q}}^\dagger a_{\mathbf{p}} \rho_Q - a_{\mathbf{p}}^\dagger a_{\mathbf{p}} - a_{\mathbf{p}-\mathbf{Q}}^\dagger a_{\mathbf{p}-\mathbf{Q}}, \quad (9)$$

spin labels being implicit in the roman characters. The indicated expectation value is expanded in a factorized-Iwamoto-Yamada (FIY) cluster expansion [26]. The individual terms in this expansion may be classified according to the number of orbital labels involved; as is customary, we will speak of "two-body," "three-body," ..., "n-body" cluster approximations when terms with more than two, more than three, ..., more than n orbital indices are neglected. Evaluation is simplified by taking the thermodynamic limit, i.e., $A \rightarrow \infty$ with ρ held constant, thus restricting the treatment to a uniform infinite system. In this manner we arrive at a cluster series of the form

$$n(\mathbf{p}, \mathbf{Q}) = n_o(\mathbf{p}, \mathbf{Q}) + (1-\delta_{Q0})[n_{(2)}(\mathbf{p}, \mathbf{Q}) + n_{(3)}(\mathbf{p}, \mathbf{Q}) + \dots]. \quad (10)$$

(We note that the similar expansion in Eq. (12) of Ref. [19] should be corrected by replacing the first term on the right, appearing as $n_F(\mathbf{p}, \mathbf{q})$, by $n_o(\mathbf{p}, \mathbf{q})$ as defined in Eq. (4) of that paper.) It is found that the generalized momentum distribution $n(\mathbf{p}, \mathbf{Q})$ is a reducible quantity, in the sense of containing factorizable contributions; however, structural relations can be given that express it in terms of sums of irreducible Ursell-Mayer diagrams [19].

In our numerical evaluation we approximate $n(\mathbf{p}, \mathbf{Q})$ to leading cluster order in the expansion (10), neglecting terms beyond $n_{(2)}$ inside the square bracket and replacing $n(p)$ in the leading term, $n_o(\mathbf{p}, \mathbf{Q})$, by the two-body cluster approximation $(\Delta n(p))_1 + (\Delta n(p))_2$ defined in Ref. [25]. This approximation to $n(\mathbf{p}, \mathbf{Q})$ is denoted $n_{LO}(\mathbf{p}, \mathbf{Q})$. The addend $n_{(2)}$ consists of a sum of seven two-body cluster terms,

$$n_{(2)}(\mathbf{p}, \mathbf{Q}) = \sum_{i=1}^7 n_{(2)}^{(i)}(\mathbf{p}, \mathbf{Q}), \quad (11)$$

represented in their turn by the Ursell-Mayer diagrams displayed in Fig. 1. (For an explanation of the relevant diagrammatic conventions, see the Appendix of Ref. [19].) The corresponding contributions to the two-body cluster component $\rho_{2(2)}(\mathbf{r}_1, \mathbf{r}_2, \mathbf{r}'_1)$ of $\rho_2(\mathbf{r}_1, \mathbf{r}_2, \mathbf{r}'_1)$ are: (12-1) $l(k_F r_{11'})\zeta(r_{12})$, (12-2) $l(k_F r_{11'})\zeta(r'_{12})$, (12-3)

$$\begin{aligned}
 & l(k_{FR11'})\zeta(r_{12})\zeta(r_{1'2}), & (12-4) & & -l(k_{FR12})l(k_{FR1'2})/v, & (12-5) \\
 & -l(k_{FR12})\zeta(r_{1'2})l(k_{FR1'2})/v, & (12-6) & & -l(k_{FR12})l(k_{FR1'2})\zeta(r_{12})/v, & \text{and } (12-7) \\
 & -l(k_{FR12})\zeta(r_{12})l(k_{FR1'2})\zeta(r_{1'2})/v, & & & \text{where } l(x) = 3x^{-3}(\sin x - x \cos x) & \text{is the Slater} \\
 & & & & \text{exchange function and } \zeta(r) = f(r) - 1 & \text{is the dynamical correlation bond.}
 \end{aligned}$$

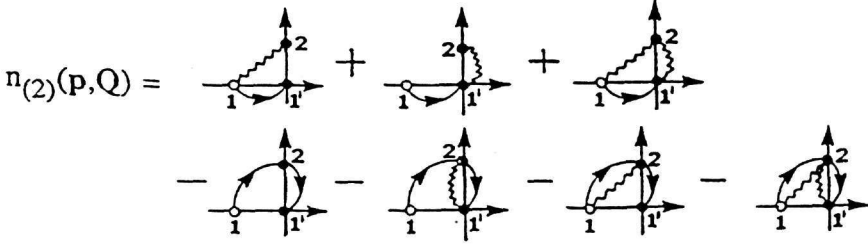


Figure 1. Diagrammatic representation of the cluster contributions $n_{(2)}^{(i)}(\mathbf{p}, \mathbf{Q}) (i=1, \dots, 7)$ to the generalized momentum distribution function. See Ref. [19].

It has been verified that the terms $n_{(2)}^{(i)}(\mathbf{p}, \mathbf{Q})$ reproduce the lowest-order parts of the addends of the highly summed structural expression derived by Ristig and Clark. This expression, Eq. (42) in Ref. [19], collects the contributions to various scattering processes in the medium. (We note incidentally that a square bracket is missing from the end of the first line of Eq. (42).) On inspection it is seen that the terms $n_{(2)}^{(1)}$ and $n_{(2)}^{(2)}$ appearing in Fig. 1 are derived from terms of Eq. (42) that describe the scattering of a nucleon from an orbital of momentum \mathbf{p} to another orbital of momentum $\mathbf{p} - \mathbf{Q}$ with the intervention of a phonon to conserve momentum, and the time-reversed counterpart of this process. The terms $n_{(2)}^{(i)}$ with $i=4, \dots, 7$ are derived from terms of Eq. (42) that describe the scattering of kinematically (i.e. Pauli-) correlated nucleons, which, however, can populate states above the Fermi sea due to the presence of dynamical correlations. Of course, the contribution $n_{(2)}^{(4)}$ coincides, for $\mathbf{Q} \neq 0$, with the generalized momentum distribution $n_F(\mathbf{p}, \mathbf{Q})$ of the ideal Fermi gas. Finally, the term $n_{(2)}^{(3)}$ is the leading portion of the addend $n^{(2)'} that acts in Eq. (42) as a correction to the simpler scattering processes.$

It is readily checked that the approximation n_{LO} as defined above preserves the following properties of the exact generalized momentum distribution: (i) it is invariant under time reversal, (ii) it satisfies the \mathbf{p} sum rule of Eq. (4), and (iii) it obeys the \mathbf{Q} sum rule

$$\sum_{\mathbf{Q}} n_{LO}(\mathbf{p}, \mathbf{Q}) = 0 . \tag{13}$$

In verifying (4), one must of course substitute the two-body cluster approximation $g_{LO}(r) = f^2(r)[1 - l^2(k_{FR})/v]$ to the radial distribution function, i.e., to the diagonal part of the two-body density. However, the approximation n_{LO} violates the condition

(6) and thus the sequential relation (5).

3. Results and Discussion

Numerical results for $n(\mathbf{p}, \mathbf{Q})$ were obtained in the lowest cluster approximation $n_{LO}(\mathbf{p}, \mathbf{Q})$ (i.e., two-body order) for three models of the ground state of symmetrical nuclear matter. These models are specified by three different correlation functions $f(r)$, all referring to densities near the saturation density of nuclear matter. One of the models is drawn from the variational Monte Carlo study of Ceperley *et al.* [27] and thus is given the designation MC. At $\rho = 0.182 \text{ fm}^{-3}$ ($k_F = 1.392 \text{ fm}^{-1}$), this model provides the correlation function

$$\text{MC} \quad f(r) = \exp[-C_1 e^{-r/C_2} (1 - e^{-r/C_3})/r] . \quad (14)$$

The parameters C_1 , C_2 , and C_3 , taken from Ref. [27], were determined by minimization of the ground-state energy expectation value of symmetrical nuclear matter with respect to the Jastrow trial function implied by (7) with (14). The assumed interaction is the v_2 "homework potential" [26,28]. This state-independent potential consists of the central part of the Reid soft-core interaction in the 3S_1 - 3D_1 channel, considered to act in all partial waves. It has been used in numerous calculations (see, for example, Refs. [28-31]) and has a repulsive core that is relatively stiff compared to those of some putatively realistic nucleon-nucleon forces. The other two models examined here, which we denote G1 and G2, are specified in terms of a Gaussian deviation of the Jastrow function $f(r)$ from unity:

$$\text{G1, G2} \quad f(r) = 1 - \exp[-\beta^2 r^2] . \quad (15)$$

These models are not derived from any known nucleon-nucleon interactions, but would naturally correspond to potentials with soft repulsive cores. They have the advantage that the integrals involved in the approximation n_{LO} may be evaluated analytically. Model G1 refers to a density $\rho = 0.1589 \text{ fm}^{-3}$ ($k_F = 1.33 \text{ fm}^{-1}$). The parameter value $\beta = 1.1 \text{ fm}^{-1}$ chosen for G1 was determined [22] by fitting a low-order calculation of the momentum distribution $n(p)$ of nuclear matter at this density to the result of a correlated-basis-functions calculation [32] of $n(p)$ for a realistic two-nucleon interaction. Model G2, specified by $\beta = 1.478 \text{ fm}^{-1}$, refers to $\rho = 0.182 \text{ fm}^{-3}$ ($k_F = 1.392 \text{ fm}^{-1}$). It has been used in a set of variational calculations of $n(p)$ intended to test various methods for numerical evaluation of the relevant correlated expectation value [29]. (These methods include the so-called LOC (lowest-order conserving), LOIC (lowest-order irreducible cluster), FHNC (Fermi-hypernetted chain), and MC (Monte Carlo) procedures.)

The use of three representative models allows us to study the effects of different aspects of the state-independent geometrical correlations on the two-body density. The

correlation functions $f(r)$ of the three models are compared in Fig. 2. Although qualitatively similar, they nevertheless show significant differences in behavior in the core region as well as at medium separations. A widely used measure of the overall strength of the dynamical correlations – which may be regarded as an estimate of their effectiveness in depleting the Fermi sea – is the wound parameter $\kappa_{\text{dir}} = \rho \int [f(r) - 1]^2 dr$. (It may be noted that the logarithm of the residue at the quasiparticle pole, as predicted by variational theory [25], is proportional to $-\kappa_{\text{dir}}$.) The values of the wound parameter for models MC, G1, and G2 are respectively $\kappa_{\text{dir}} = 0.297, 0.237, \text{ and } 0.111$, indicating that these models span a range from relatively strong to relatively weak correlations.

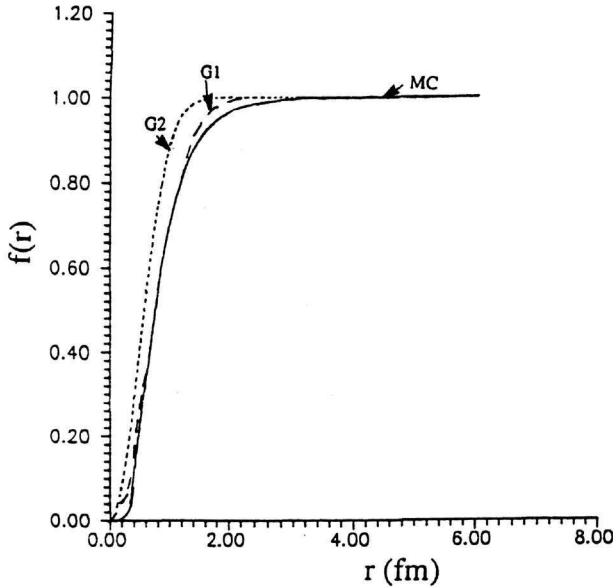


Figure 2. The correlation functions $f(r)$ of the three models MC, G1, and G2 (see text).

Some of the results of our numerical study are presented in Figs. 3-11. The ranges $p \in [0, 3k_F]$ and $Q \in (0, 5k_F]$ have been considered for the magnitudes of the momenta involved. Attention is restricted to $Q \neq 0$. We first discuss the results for model MC in the case that \mathbf{p} and \mathbf{Q} are parallel. The approximation $n_{\text{LO}}(\mathbf{p}, \mathbf{Q})$ to the generalized momentum distribution $n(\mathbf{p}, \mathbf{Q})$ is shown in Figs. 3 and 4, while Figs. 5, 6, and 7 display the respective individual terms $n_{(2)}^{(2)}$ (which is just the ideal Fermi gas result), $n_{(2)}^{(1)}$, and $n_{(2)}^{(3)}$. For the perfect Fermi gas, $n(\mathbf{p}, \mathbf{Q}) (= n_{(2)}^{(2)}$ for $Q \neq 0$) is simply -1 for $p \leq k_F$ and $0 \leq Q \leq p + k_F$, and zero otherwise. In Figs. 3 and 4 the full $n_{\text{LO}}(\mathbf{p}, \mathbf{Q}) = n_{(2)}(\mathbf{p}, \mathbf{Q})$ is seen to increase monotonically with Q for $Q \leq p + k_F$, starting from substantial negative values at small Q . At $Q = p + k_F$, this function exhibits an abrupt rise toward zero. When the momentum variable Q is in the range $0 \leq Q \leq p + k_F$, the terms $n_{(2)}^{(1)}$,

$n_{(2)}^{(2)}$, and $n_{(2)}^{(4)}$ make the contributions to $n_{LO}(\mathbf{p}, Q\mathbf{p}/p)$ of largest magnitude; the terms $n_{(2)}^{(2)}$, $n_{(2)}^{(6)}$, and $n_{(2)}^{(3)}$ are somewhat less important; and $n_{(2)}^{(7)}$ has little consequence. The deviation of $n_{LO}(\mathbf{p}, Q\mathbf{p}/p)$ from zero in the region $Q > p + k_F$ is entirely due to the presence of dynamical correlations. Among the contributing terms, $n_{(2)}^{(2)}$, $n_{(2)}^{(6)}$, and $n_{(2)}^{(3)}$ are comparable, while $n_{(2)}^{(7)}$ is again of small magnitude. Dynamical correlations are also responsible for the departure of the estimated $n(\mathbf{p}, \mathbf{Q})$ from zero at values of p beyond k_F . In this regime, and Q satisfying $|p - k_F| \leq Q \leq p + k_F$, it is $n_{(2)}^{(1)}$ and next $n_{(2)}^{(2)}$ that give the leading contributions, followed by $n_{(2)}^{(3)}$ and $n_{(2)}^{(2)}$. These last two terms also contribute in the region $Q > p + k_F$. The various orderings we have indicated are generally understandable in terms of the number of correlation lines (the wavy lines representing ζ factors) involved in the corresponding diagrams, as well as the respective factors in ρ and inverse degeneracy $v^{-1}=1/4$.

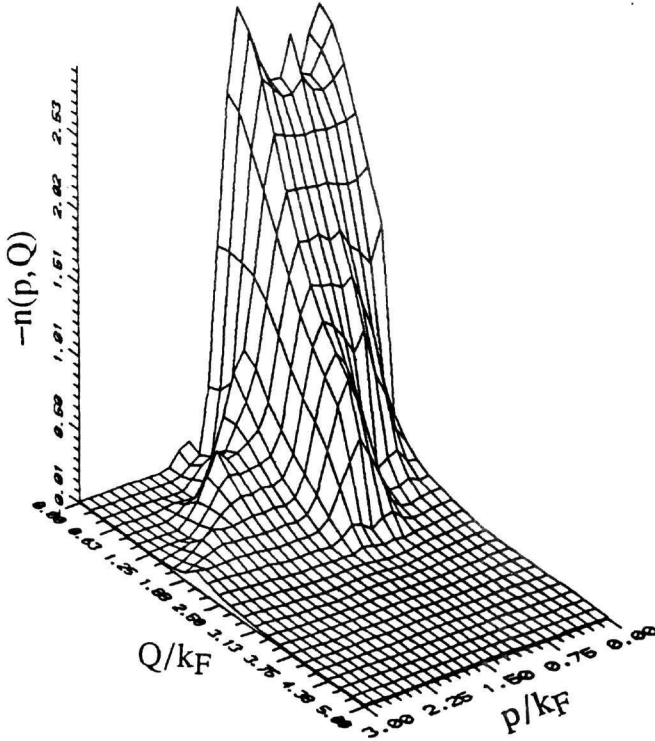


Figure 3. The lowest-order generalized momentum distribution $n_{LO}(\mathbf{p}, \mathbf{Q})$ as a function of p and Q for \mathbf{p} parallel to \mathbf{Q} and $Q \neq 0$, calculated with the MC correlation function of Ref. [27].

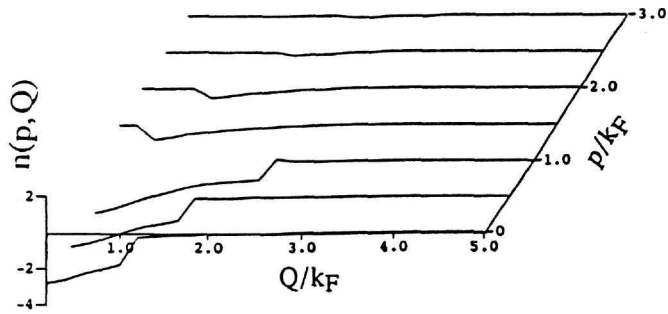


Figure 4. A different view of the data of Figure 3.

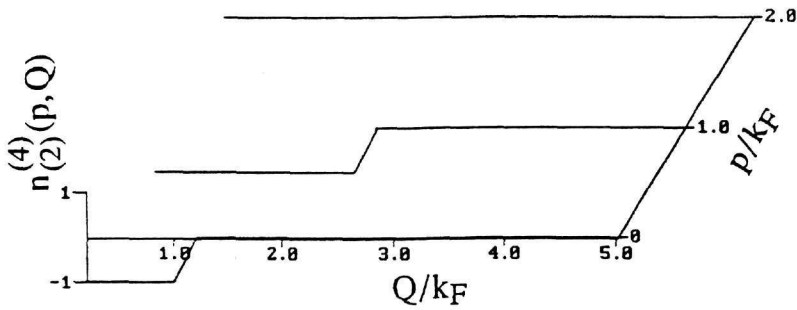


Figure 5. The term $n_{(2)}^{(4)}$ as a function of p and Q for \mathbf{p} parallel to \mathbf{Q} ($\rho = 0.182 \text{ fm}^{-3}$).

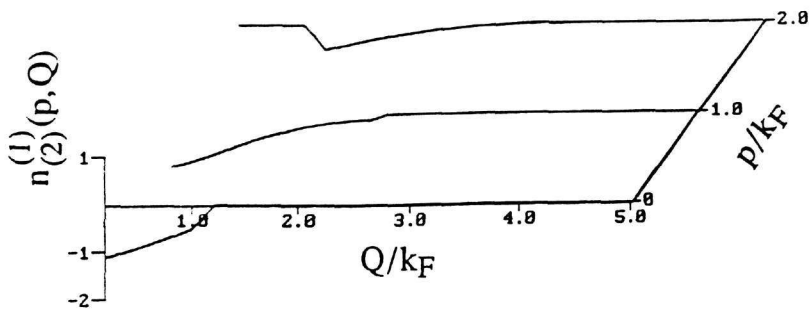


Figure 6. The term $n_{(2)}^{(1)}$ as a function of p and Q for \mathbf{p} parallel to \mathbf{Q} , obtained with the MC correlation function of ref. [27] ($\rho = 0.182 \text{ fm}^{-3}$).

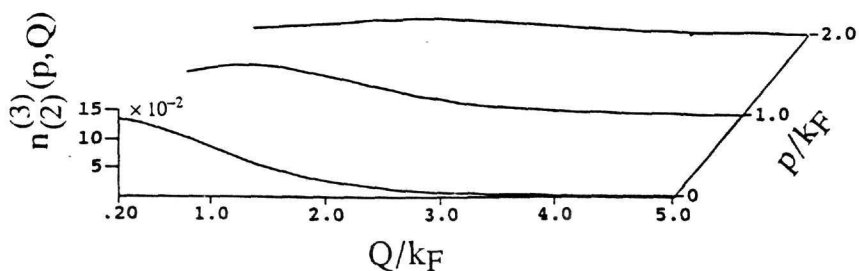


Figure 7. Same as Figure 6, for the term $n_{(2)}^{(3)}$.

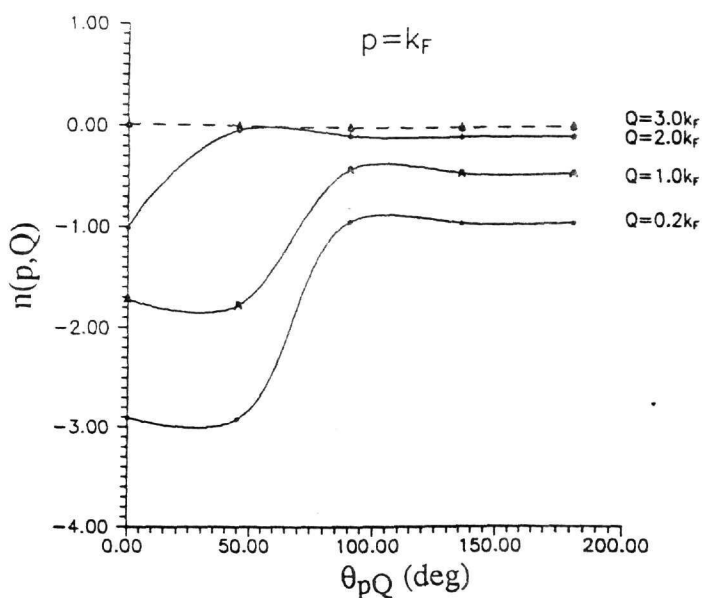


Figure 8. The lowest-order generalized momentum distribution $n_{LO}(\mathbf{p}, \mathbf{Q})$ as a function of the angle $\theta_{\mathbf{p}\mathbf{Q}}$ between \mathbf{p} and \mathbf{Q} obtained at several Q values ($Q \neq 0$) for $p = k_F$ with the MC correlation function of ref. [27] ($\rho = 0.182 \text{ fm}^{-3}$). (The numerical results are plotted as small triangles; the curves have been drawn merely to guide the eye.)

Information on the dependence of our estimate of $n(\mathbf{p}, \mathbf{Q})$ on the angle $\theta_{\mathbf{p}\mathbf{Q}}$ between \mathbf{p} and \mathbf{Q} is furnished by Fig. 8 for the case $p = k_F$ at selected values of Q . For all four choices of Q , we find that $n_{LO}(\mathbf{p}, \mathbf{Q})$ is at or very close to its minimum value when $\theta_{\mathbf{p}\mathbf{Q}}$ is zero, i.e., when \mathbf{p} and \mathbf{Q} are parallel. For $Q \leq 2k_F$ this quantity is seen to increase at small angles and then flatten out at large $\theta_{\mathbf{p}\mathbf{Q}}$. Similar behavior has been observed at other values of p .

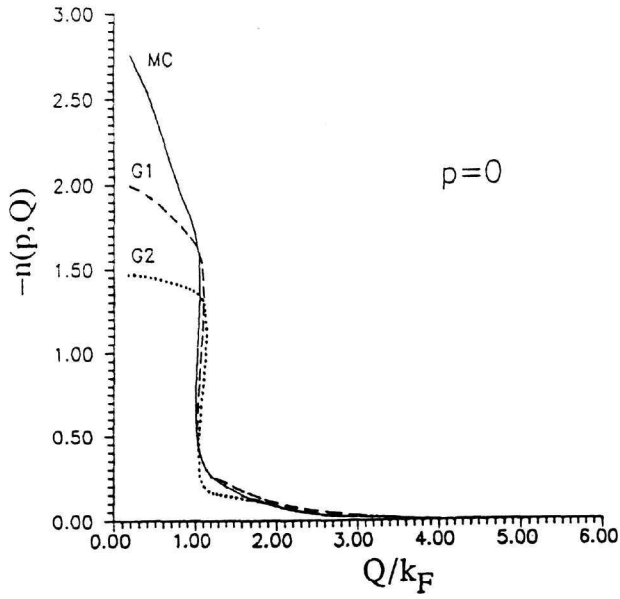


Figure 9. The lowest-order generalized momentum distribution $n_{LO}(p, Q)$ as a function of Q ($Q \neq 0$) for p equal 0, for the three models MC, G1, and G2.

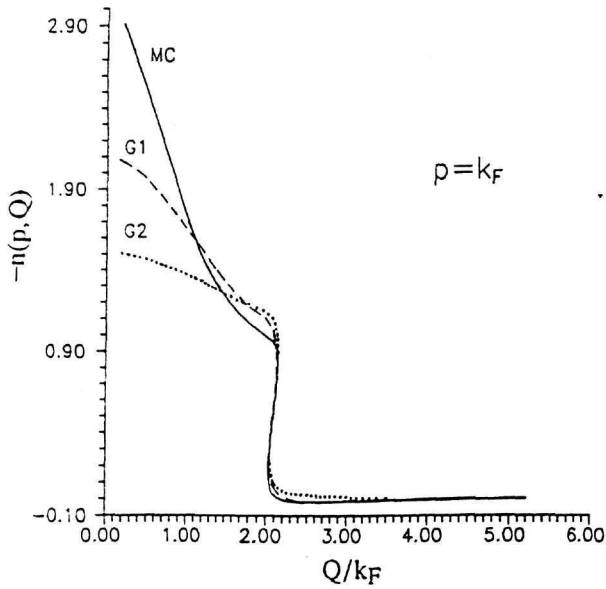


Figure 10. The lowest-order generalized momentum distribution $n_{LO}(p, Q)$ as a function of Q ($Q \neq 0$) for p equal k_F and p parallel to Q , for the three models MC, G1, and G2.

The dependence of the results on the choice of correlation function is illustrated in Figs. 9-11, for $\theta_{pQ} = 0$ and three characteristic values of p , namely 0, k_F , and $2k_F$. Qualitatively, the predictions of MC, G1, and G2 models are similar, although substantial differences do arise at small or intermediate Q values. A more quantitative observation, holding as a general statement with minor qualifications, is that in the regions where significant disagreements between the three models are seen, the magnitude of $n_{LO}(p, Q)$ increases with the size of the wound parameter κ_{dir} . As is to be expected, the deviation of $n_{LO}(p, Q)$ from the generalized momentum distribution of the ideal Fermi gas is also generally larger for larger κ_{dir} , as is the violation of the sequential relation. The predictions of the three models appear to merge for large values of Q (i.e. for $Q > p + k_F$).

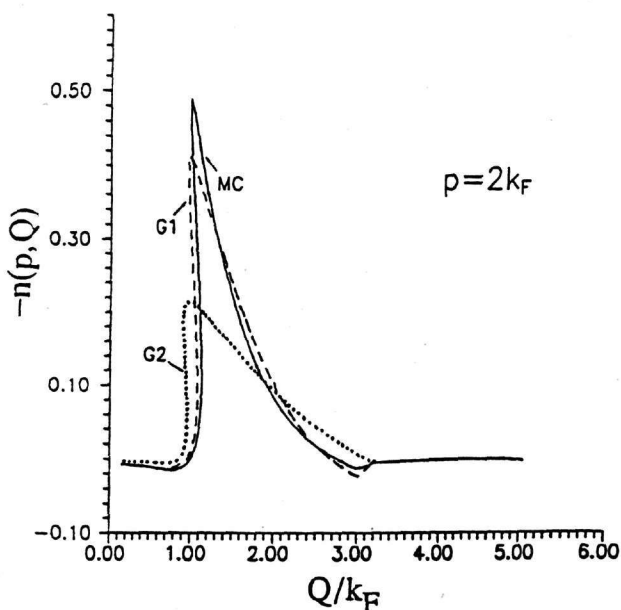


Figure 11. As in Figure 10, but for $p = 2k_F$.

For the MC model, we have compared our results with Silver's approximation [17b] to the generalized momentum distribution, given by $n(p, Q) = n(p)[S(Q) - 1]$. As inputs to this simple expression we use the momentum distribution $n(p)$ and static structure function $S(Q)$ from a FHNC calculation for the MC correlation function at the relevant density. The Silver estimate yields substantially smaller values of $|n(p, Q)|$ than the leading cluster approximation to this quantity, in the "Fermi-gas" region of nonvanishing $\Theta(k_F - p)\Theta(k_F - |p - Q|)$.

4. Conclusions

In summary, we have reported selected results from a study of the half-diagonal two-body density matrix $\rho_2(\mathbf{r}_1, \mathbf{r}_2, \mathbf{r}'_1)$ in symmetrical nuclear matter. The results have been framed in terms of the Fourier transform $n(\mathbf{p}, \mathbf{Q})$ of $\rho_2(\mathbf{r}_1, \mathbf{r}_2, \mathbf{r}'_1)$, the so-called generalized momentum distribution [18,19]. Our study is based on a Jastrow ansatz for the ground-state wave function, and we have discussed various aspects of the numerical findings for three versions of the state-independent Jastrow two-body correlation function $f(r)$, at densities near the experimental equilibrium density of the system. Although the results show interesting and possibly significant structural features, this effort constitutes only the first attempt at quantitative calculation of $n(\mathbf{p}, \mathbf{Q})$ for infinite nuclear matter and thus will be subject to many refinements.

Several considerations suggest that higher-order cluster corrections may play a more important role in the treatment of $n(\mathbf{p}, \mathbf{Q})$ than has been found to be the case for the analogous one-body quantity, the momentum distribution $n(p)$ [29]. In particular, we may point to (i) the large deviations of the predictions for $n(\mathbf{p}, \mathbf{Q})$ at $Q \neq 0$ from the result for the noninteracting Fermi gas, (ii) the failure of the sequential relation, which can assume serious magnitude, and (iii) the sensitivity of these deviations and violations to the size of the wound parameter κ_{dir} . It is of course anticipated that cluster convergence will be worse, the larger the value of κ_{dir} ; however, in the present context it appears that the generally larger quantity $|\rho \int \zeta(r) dr| = |\rho \int [f(r) - 1] dr|$ may serve as a more appropriate "smallness parameter" for measuring the rapidity of cluster convergence. We are currently investigating three alternatives to improvement of the present evaluation of $n(\mathbf{p}, \mathbf{Q})$. In the first, we form a simple approximation (called LOC, in analogy to the so-called lowest-order conserving approximation to the momentum distribution [29]) by retaining the leading nontrivial cluster terms beyond $n_{\text{LO}}(\mathbf{p}, \mathbf{Q})$ that are needed to ensure satisfaction of the sequential relation (or equivalently, condition (6)). The other two procedures are based on the structural relation for $n(\mathbf{p}, \mathbf{Q})$ derived by Ristig and Clark [19] (their Eq. (42)). These procedures involve summation of selected cluster diagrams from all orders of the expansion (10). The simpler approach keeps only the leading cluster contributions to the irreducible quantities in terms of which $n(\mathbf{p}, \mathbf{Q})$ is expressed (called the LOIC approximation, after the lowest-order irreducible cluster prescription of Ref. [29]). Preliminary results from this approach are in accord with the expectation that it will display better convergence properties than the straightforward cluster expansion considered herein. In a more elaborate treatment we plan a full FHNC/O calculation of $n(\mathbf{p}, \mathbf{Q})$, which will provide a firm basis for assessing the efficacy of the more naive approximations.

Although FHNC evaluation is clearly the "method of choice" from the standpoint of accurate determination of the generalized momentum distribution $n(\mathbf{p}, \mathbf{Q})$ for a Jastrow wave function, the formulation and testing of simple analytic or semi-analytic approximations remains a desirable goal, since it may be possible to adapt them easily

to the presence of state-dependent correlations and for phenomenological analyses of FSI in finite nuclei. A similar strategy has proven successful in the case of the ordinary momentum distribution [22].

We have discussed above some extensions of the present work that are designed to improve convergence and achieve a quantitatively reliable description of the two-body density matrix, insofar as state-independent correlations play the dominant role. However, it is doubtless the case that a truly realistic description of $\rho_2(\mathbf{r}_1, \mathbf{r}_2, \mathbf{r}'_1)$ and $n(\mathbf{p}, \mathbf{Q})$ over the full range of the spatial and momentum variables will require the introduction of state-dependent (spin-, isospin-, and angle-dependent) correlations into the trial ground-state wave function of nuclear matter [34,35]. As an important step in this direction, the formalism developed by Ristig and Clark [18,19] should be generalized to deal with correlation operators appropriate to a nucleon-nucleon interaction of v_6 type [26,35].

Acknowledgements

This research has been supported in part by the Physics Division and the Division of Materials Research of the U. S. National Science Foundation under Grant No. PHY/DMR-9002863. E. M. thanks the University of Athens for partial financial support for a recent visit to Washington University, where she enjoyed the hospitality of the Department of Physics and the McDonnell Center for the Space Sciences. She is also grateful to W. H. Dickhoff, V. R. Pandharipande, and R. Seki for very helpful discussions. We thank M. F. Flynn for providing FHNC data for $n(p)$ and $S(Q)$.

References

- [1] B. Frois and C. Papanicolas, *Ann. Rev. Nucl. Part. Sci.* **37** (1987) 133; D. B. Day *et al.*, *Ann. Rev. Nucl. Part. Sci.* **40** (1990) 357.
- [2] D. K. A. De Witt Huberts, *J. Phys.* **G16** (1990) 507; D. F. Geesaman *et al.*, *Phys. Rev. Lett.* **63** (1989) 734; G. Garino *et al.*, *Phys. Rev.* **C45** (1991) 780; NE.18 experiment, SLAC, under analysis; Letter of Intent, SLAC End Station A, Nov. 1991.
- [3] A. S. Carroll *et al.*, *Phys. Rev. Lett.* **61** (1988) 1698; Brookhaven AGS proposal E850, A.S.Carroll and S. Heppelmann, spokespersons.
- [4] D. Ashery and J. Schiffer, *Ann. Rev. Nucl. Part. Sci.* **36** (1986) 207.
- [5] O. Benhar *et al.*, *Phys. Rev.* **C44** (1991) 2328.
- [6] A. Kohama, K. Yazaki and R. Seki, to appear in *Nucl. Phys. A*.
- [7] J. W. Clark and R. N. Silver, in *Proceedings of the Third International Conference on Nuclear Reaction Mechanisms*, ed. E. Gadioli (Università degli Studi di Milano, 1988), p. 531 and references therein.

- [8] C. Ciofi degli Atti, E. Pace and G. Salme, Phys. Rev. C43 (1991) 1155.
- [9] A. S. Rinat and W. H. Dickhoff, Phys. Rev. B42 (1990) 10004.
- [10] S. Stringari, Phys. Rev. B46 (1992) 2974 and references therein.
- [11] E. Feenberg, *Theory of Quantum Fluids* (Academic Press, New York, 1969).
- [12] J. W. Clark and M. L. Ristig, in *Momentum Distributions*, eds. R. N. Silver and P. E. Sokol (Plenum Press, New York, 1989), p. 39 and references therein.
- [13] O. Benhar, A. Fabrocini and S. Fantoni, Nucl. Phys. A505 (1989) 267; Phys. Rev. C41 (1990) R24; and to be published.
- [14] B. E. Vonderfecht, W. H. Dickhoff, A. Polls and A. Ramos, Phys. Rev. C44 (1991) R1265.
- [15] C. Mahaux and R. Sartor, Phys. Rep. 211 (1992) 53.
- [16] A. N. Antonov, P. E. Hodgson and J. Zh. Petkov, in *Nucleon Momentum and Density Distributions in Nuclei*, (Clarendon Press, 1988).
- [17] (a) H. A. Gersch, L. J. Rodriguez and P. N. Smith, Phys. Rev. A5 (1972) 1547; (b) R. N. Silver, Phys. Rev. B38 (1988) 2283; (c) A. S. Rinat, Phys. Rev. B40 (1989) 6625.
- [18] M. L. Ristig and J. W. Clark, Phys. Rev. B40 (1989) 4355.
- [19] M. L. Ristig and J. W. Clark, Phys. Rev. B41 (1990) 8811.
- [20] D. M. Ceperley, in *Momentum Distributions*, eds. by R. N. Silver and P. E. Solol (Plenum, New York, 1989), p. 71.
- [21] C. Carraro and S. E. Koonin, Nucl. Phys. A524 (1991) 201; C. Carraro, R. Seki and T. Shoppa, unpublished.
- [22] S. Stringari, M. Traini and O. Bohigas, Nucl. Phys. A516 (1990) 33.
- [23] E. Mavrommatis, M. Petraki and J. W. Clark, in *Proceedings of the Second Hellenic Symposium on Theoretical Nuclear Physics 1991*, eds. M. Anagnostatos, et al. (University of Athens and NCSR Demokritos, 1992), p. 15
- [24] We use here Q instead of q of references [18,19]. Notice that Q has been also used for the four-momentum transfer.
- [25] M. L. Ristig and J. W. Clark, Phys. Rev. B14 (1976) 2875.
- [26] J. W. Clark, in *Progress in Particle and Nuclear Physics*, ed. D. H. Wilkinson (Pergamon, Oxford, 1979), Vol. 2, p. 89.
- [27] D. Ceperley, G. V. Chester, and M. H. Kalos, Phys. Rev. B16 (1977) 3081.
- [28] V. R. Pandharipande, R. B. Wiringa and B. D. Day, Phys. Lett. B57 (1975) 205.
- [29] M. F. Flynn et al., Nucl. Phys. A427 (1984) 253.
- [30] A. Ramos, A. Polls and W. H. Dickhoff, Nucl. Phys. A503 (1989) 1.

- [31] E. Mavrommatis and J. W. Clark, in *Condensed Matter Theories*, ed. V. C. Aguilera-Navarro (Plenum Press, New York, 1990), Vol. 5, p. 97.
- [32] S. Fantoni and V. R. Pandharipande Nucl. Phys. A**427** (1984) 473.
- [33] Notice in Fig. 11 the difference in scale.
- [34] M. L. Ristig, W. J. Ter Louw and J. W. Clark, Phys. Rev. C**3** (1971) 1501; Phys. Rev. C**5** (1972) 695.
- [35] V. R. Pandharipande and R. B. Wiringa, Rev. Mod. Phys. **51** (1979) 821.